Kinematics of Eley-Rideal Reactions at Hyperthermal Energies

Yunxi Yao[1] and Konstantinos P. Giapis[1*]

Division of Chemistry and Chemical Engineering, California Institute of Technology, Pasadena, California 91125, USA
(Received 18 February 2016; published 21 June 2016)

Direct or Eley-Rideal reactions between energetic N^+ and O^+ projectiles and O atoms, adsorbed onto Pt and Pd surfaces, are studied experimentally at incidence energies between 20 and 200 eV. The exit energies of the diatomic molecular products NO and O_2 depend linearly on the incidence energy of the corresponding projectiles. A reaction mechanism is proposed, where the incident projectile collides with a single metal atom on the surface, linked to an adsorbed O atom. At the apsis point, a high-energy transient state is formed between the projectile, substrate, and adsorbate atoms. As the projectile begins to rebound, the transient state decomposes into a diatomic molecule, consisting of the original projectile and the adsorbed O atom, which exits the surface with memory of the incidence energy. Energy and momentum conservation during this single-bounce event (atom in, molecule out) accurately predict the exit energy of the molecular product, thus capturing the kinematics of the direct reaction.

Gas-surface reactions are often thought to proceed between two extremes: the Langmuir-Hinshelwood (LH) mechanism, which requires all reactants to be adsorbed onto and in thermal equilibrium with the surface, and the Eley-Rideal (ER) mechanism, where an energetic reactant (the "projectile") impinges onto a surface adsorbate and bonds with it directly [1]. The LH mechanism applies to most surface chemical reactions and is well understood [2]. The ER mechanism is still being debated: the rarity of chemical environments where hyperthermal reactive species bombard surfaces, combined with experimental difficulties in detecting energetic reaction products, has impeded progress in understanding such reactions. In fact, even the definition of an ER reaction is outright crude: the notion of a bond forming between an energetic projectile and a surface adsorbate in a *head-on* collision, followed up by ejection from the surface of an energetic reaction product, violates momentum conservation. This problem does not arise if the projectile collides first with the surface. Hot atom reactions represent an intermediate mechanism, where the projectile undergoes few bounces before reacting with an adsorbate [3]. Owing to multiple collisions, which lead to variable energy losses, these do not qualify as prompt ER reactions.

What comprises an ER reaction? The literature consensus suggests that ER reactions should have at least the following attributes: (i) they require a gas-phase projectile with high kinetic or potential energy, impinging onto an adsorbate-covered surface; (ii) they yield a fast-moving molecular product, consisting of the projectile-adsorbate combination, which leaves the surface (no trapping); and (iii) the product translational energy must be directly correlated to the energy of the incident projectile. Secondary attributes include that (iv) the product molecule may be internally excited; and (v) the product angular flux distribution deviates from the cosine law, with subspecular preference for off-normal incidence angles.

Several reports of fast molecular products, observed in hyperthermal gas-surface collisions, have uncovered key attributes of direct reactions. The first claim of an ER reaction involved the hydrogenation of fast $N(C_2H_4)_3N$, scattering off of H-covered Pt(111) [4]. Next, HD molecules were shown to form by an ER reaction between energetic H(D) projectiles and D(H) atoms adsorbed onto a Cu(111) surface; the HD product exhibited asymmetrical angular flux distribution, which varied with the incidence energy [5]. The vibrational and rotational state distribution of the HD products was subsequently resolved [6,7]. Both ER and LH reaction mechanisms were shown to occur simultaneously in the formation of HCl from energetic H atoms and Cl adsorbed on Au(111), which established that product exit energy and angular flux distribution offer means for distinguishing between the two mechanisms [8]. These studies have employed hydrogen atoms as adsorbates and/or projectiles, perhaps because the reaction exothermicity can release enough kinetic energy to the molecular product to prevent surface trapping [6,7,9–12].

ER reactions with heavier projectiles or adsorbates were demonstrated in O-atom abstraction by O^+ and NO^+ ions on oxidized Si(100) [13,14]. The formation of fast molecular F_2^- products with energies up to 90 eV was reported for hyperthermal F^+ ion abstraction of adsorbed F atoms on Ag and Si surfaces [15]. Recently, the abstraction of adsorbed O and N atoms on Ru(0001) was shown with an effusive beam of neutral nitrogen species $(N + N_2)$ [16]. In computational studies of N-atom abstraction by energetic N on Ag(111), ER reactions were shown to be highly efficient [17]. Most of these studies focused on proving that the molecular product is indeed produced by an ER reaction. No attempt has been made to show how the product is

formed, how energy is dissipated, or how to quantify the kinetic energy of the exiting product.

Despite the interest in ER reactions, a concise mechanism has yet to emerge. The present Letter focuses on the collision kinematics, a crucial part of a dynamic mechanism. Ions are used as incident projectiles because the charge allows for the creation of isotopically pure beams with precise control of the kinetic energy. Scattering at hyperthermal energies enables surface ionization [5], a process that permits the facile detection of products as ions. Relying on ions simplifies experimental measurements but adds interpretational complexity as one must account for surface neutralization and reionization with concomitant inelastic energy losses [18].

Experiments were conducted in a scattering apparatus [15,19] with mass-selected and energy-tuned hyperthermal N^+ and O^+ ion beams interacting with O atoms adsorbed onto Pt and Pd surfaces. The ion beams were extracted from a plasma discharge, operating at 5 mTorr with a feed of $N_2/Ar/Ne$ and $O_2/Ar/Ne$ mixtures, respectively. Pure atomic ion beams were delivered to grounded polycrystalline metal surfaces (Pt, Pd), held at room temperature, at currents between 2 and 5 μA over a 7 mm^2 area. The scattering geometry was set at 45° incidence and 45° exit. The surfaces were sputter cleaned and continuously dosed with O_2, known to dissociate spontaneously on Pt and Pd [20,21], thus replenishing abstracted O atoms and providing a stable steady-state coverage (O_2 pressure dependent). Fast molecular NO and O_2 products, exiting the surface as ions, were mass analyzed with a quadrupole mass spectrometer (Extrel QPS); their exit energy was measured with an electrostatic energy analyzer at a constant pass energy of 15 eV. Both positive and negative ions were eventually counted [22] with a channeltron, biased accordingly. Signal intensity was normalized to the beam current measured on the sample.

Figures 1(a) and 1(b) show the scattering spectra for NO^+ and NO^- ions, formed when a 103 ± 3 eV beam of N^+ is directed onto a Pd surface at various background O_2 pressures. Before O_2 dosing, there is no signal. Upon O_2 exposure, however, fast molecular NO ions of both polarities are clearly observed exiting the surface, even at 1×10^{-8} Torr of O_2. The main NO^+ and NO^- peaks, centered at 61.2 and 58.1 eV, respectively, account for a considerable fraction of the N^+ incidence energy. These exit energies are independent of background O_2 pressure. Above 1×10^{-7} Torr, weak and broad NO^+ scattering signal is also detected at ~20 eV, an energy typical of surface sputtering. Clearly, the fast molecular ions are not a result of sputtering. Their appearance is contingent on having an energetic N^+ projectile interacting with a surface partially covered with O atoms. Thus, the first and second requirements for an ER reaction are met.

The third requirement stipulates that the molecular ion product have memory of the projectile kinetic energy. This is
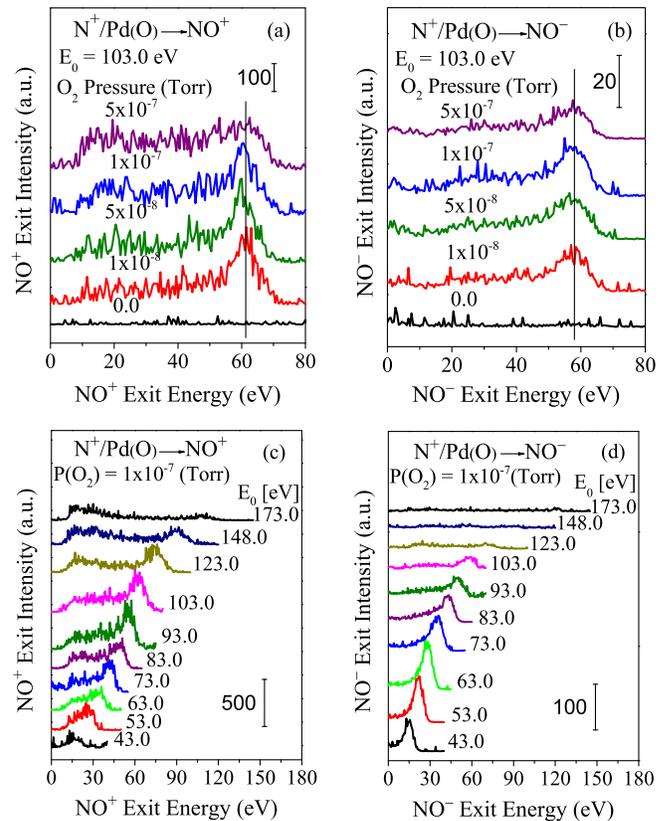

FIG. 1. Energy distributions of (a) NO^+ and (b) NO^- ion exits for $N^+/Pd(O)$, at fixed $E_0 = 103 \pm 3$ eV, for various background O_2 exposures as indicated. Energy distributions of (c) NO^+ and (d) NO^- ion exits for $N^+/Pd(O)$, exposed to O_2 at 1×10^{-7} Torr, for multiple N^+ incidence energies as indicated.

indeed the case as it can be verified from a survey of NO^+ and NO^- exit energy spectra as a function of the N^+ incidence energy, shown in Figs. 1(c) and 1(d). Both ion exits exhibit dynamic scattering peaks, which shift monotonically with incidence energy. Can this exit energy be predicted?

The well-defined NO^+/NO^- peaks at different energies can potentially reveal the kinematics of the ER reaction. Insight can be obtained with a surface collision scenario in mind. Figure 2 depicts schematically our working model for the collision sequence, which has three steps. (i) Projectile P (atomic mass, m_P) approaches a substrate atom S (m_S) linked to an adsorbate A (m_A). (ii) At the distance of closest approach (apsis) between P and S, a transient state PSA forms, with both P and A linked to the substrate atom S. The transient state is extremely short lived, but allows for a link to form between the projectile and adsorbate. (iii) The transient state decomposes, producing a fast molecular product PA, which exits the surface.

The ER reaction is then modeled as an "atom-in, molecule-out" single-collision event,

$$P + AS \rightarrow PA + S.$$
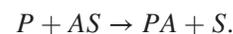
In this scenario, energy is transferred predominantly to the substrate atom during the hard collision. The incidence energy is partitioned between the substrate atom and the molecular product. Alternatively, one can assume that an impulsive potential builds up during the hard collision, which releases energy into the molecular product exiting the surface. Since the incidence energy is much larger than typical bond energies, we may neglect the latter and assume

that both energy and momentum are conserved during the single collision.

The conservation equations [23] can easily be combined to derive the kinematic factor for the ER reaction product, defined as $K(\theta) = E_e/E_0$, where θ is the deflection angle, and E_e and E_0 denote the kinetic energy of the exiting product PA and incident projectile P, respectively,

$$K(\theta) = \frac{\left[\sqrt{m_P(m_P + m_A)}\cos\theta \pm \sqrt{(m_P + m_A + m_S)(m_S - m_P) + m_P(m_P + m_A)\cos^2\theta}\right]^2}{(m_P + m_A + m_S)^2}. \qquad (1)$$

When $\theta = 90°$, as in the experiments performed here, the kinematic factor becomes

$$K(90°) = (m_S - m_P)/(m_P + m_A + m_S). \qquad (2)$$

This expression deviates from standard binary collision theory (BCT) [24] because the exiting species is the molecular product instead of just the projectile. However, $K(90°)$ converges to the BCT value for a projectile exit when $m_A \ll (m_P + m_S)$, that is, when the adsorbate is very light. Thus, in direct abstraction reactions of adsorbed hydrogen atoms, the kinematics of the product molecule should be indistinguishable from those of the exiting projectile (binary interaction). For heavier adsorbates such as O atoms, the ER reaction product (e.g., NO or O_2) should have much lower kinetic energy vs the scattering projectile itself (N or O), despite the larger mass of the former. This simple prediction is verified below for $O^+/Pd(O)$, by comparing the scattered O^- projectile to the O_2^- product.

Figure 3(a) summarizes the exit energies of both NO^+ and NO^- as a function of N^+ incidence energy. A linear

dependence is obvious for both products. Applying Eq. (2) to $N^+/Pd(O)$, a kinematic factor of 0.6784 is obtained, which captures the slopes of both NO^+ and NO^- exit energy data exceptionally well [see Fig. 3(a)]. This surprising result lends credibility to the single-collision basis of the proposed ER reaction mechanism. The linear fitting yields a negative intercept, which indicates additional (inelastic) energy losses occurring during the surface collision, reaction, and charge transfer process.

Further confirmation for the role of the substrate atoms is obtained by changing the scattering surface (See Supplemental Material [25]). The NO^+ and NO^- exit energies obtained for $N^+/Pt(O)$ are summarized in Fig. 3(b). Applying Eq. (2) yields a kinematic factor of 0.8044, indicating a more energetic product exit from the more massive Pt, consistent with single-bounce scattering, where the substrate atom controls the impulsive energy transfer. This kinematic factor captures again very well the slope of both NO^+ and NO^- exit energy data for scattering
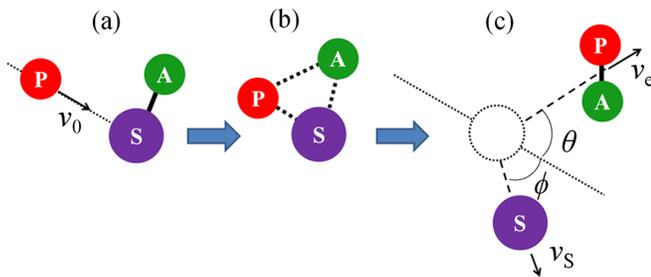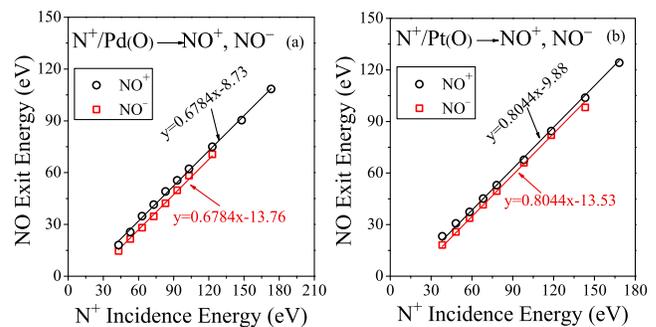

FIG. 2.   Schematic depiction of the collision sequence for the proposed Eley-Rideal reaction mechanism: (a) approach, (b) formation of a triatomic transient state at the distance of closest approach, and (c) rebound and molecular product formation. The product molecule (PA) is formed during a single collision between the projectile (P) and a substrate atom (S), linked to an absorbate atom (A). The collision geometry and velocities of the various reaction participants are indicated in (c).

FIG. 3.   Exit energies of NO^+ and NO^- as a function of N^+ incidence energy after scattering on (a) Pd and (b) Pt polycrystalline surfaces, exposed to a background of O_2 at 1×10^{-7} and 5×10^{-7} Torr, respectively. The open symbols are experimental data. The solid lines are linear fittings with fixed slopes calculated from binary collision theory. The only adjustable parameter in each fitting is the intercept value, which indicates cumulative inelastic energy loss during the collision. The correlation coefficient (R^2) for all fittings was ≥0.997.

on Pt. Despite the difference in kinematic factors between the two surfaces, the fitting of the Pt data produces almost the same intercept as the Pd data, suggesting that the inelastic energy losses are independent of the nature of the metal surface.

We note here that no scattered atomic N ions are observed from either Pd or Pt, which suggests 100% neutralization of the incident N^+ ions during the collision. Thus, the ER reaction is occurring between an incident *neutralized* N atom and an adsorbed O atom. The detected NO^+ and NO^- ions must therefore be produced at or near the surface by different charge transfer mechanisms. This is manifested in the larger kinetic energy of NO^+ vs NO^-, regardless of the surface. Stated otherwise, the inelastic energy loss is larger for NO^- formation. Under equilibrium conditions, negatively charged molecular ions can form by resonant attachment of electrons emitted from the metal surface due to lowering of the electron affinity level by the image charge effect [26], schematically depicted in Fig. 4. This effect works in reverse for positive ions, causing a rise in the ionization level [26]. Resonant ionization of a molecule near the surface becomes possible when the ionization level overlaps with the metal Fermi level. Whether overlap occurs depends on the ionization energy (IE) of the molecule, the metal work function (ϕ), and the apsis. The reaction barriers for positive and negative ion formation by resonant charge transfer are $IE - \phi$ and $\phi - EA$, respectively, where EA denotes the electron affinity of the scattered molecule. The work functions

for polycrystalline Pd and Pt are 5.22 and 5.64 eV, respectively [27]. The IE and EA of NO are 9.26 and 0.026 eV, respectively [28]. Then, the reaction barriers for forming NO^+ and NO^- by charge transfer on Pd are calculated to be 4.0 and 5.2 eV, respectively. Since the energy for forming these ions must originate in the incidence kinetic energy, the larger reaction barrier for forming NO^- implies that less energy is available to the exiting NO^- vs NO^+. From this reasoning, the NO^+ product should possess a larger kinetic energy than NO^- by about 1.2 eV. This is indeed observed, albeit the difference in intercepts of 5 eV suggests additional inelastic losses [29]. The same argument applies also to the Pt surface, where the reaction barriers for NO^+ and NO^- formation are calculated to be 3.6 and 5.6 eV, respectively. Here, the predicted difference in kinetic energy between NO^+ and NO^- of 2.0 eV is closer to the intercept-derived value of 3.7 eV.

The proposed mechanism was further validated by analyzing the kinematics of reactions between incident O^+ ions and adsorbed O atoms [25]. In this symmetric reaction system, the surface is partially covered with O atoms originating from the O^+ beam, which obviates the need for O_2 dosing. Excepting sputtering peaks of O^+, which appear at ~20 eV for high incidence energies (≥ 100 eV), no dynamically scattered O^+ ions are detected. Instead, O^- ions are exclusively observed exiting both Pd and Pt surfaces. In addition, fast O_2^- and O_2^+ ions are clearly produced, although the O_2^+ signal is very weak. These molecular ions exhibit similar dynamic behavior to the NO ions, formed with the N^+ beam. The exit energies of O^-, O_2^-, and O_2^+ are plotted in Fig. 5, as a function of O^+ incidence energy. The energetics of O^- and O_2^- exhibit good linear dependence, while that of O_2^+ is less well described (noisy signal). The calculated kinematic factor for O exits from O^+/Pd is 0.7386, which fits the O^- energy data very well. This observation provides further support for single-bounce scattering, where a fraction of the
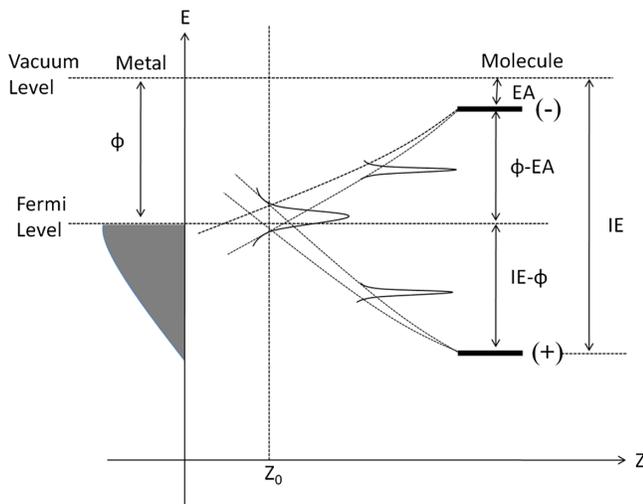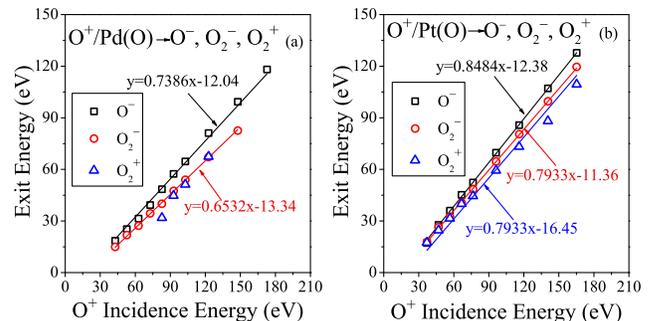
FIG. 4. Schematic depiction of the evolution of a vacant electron state (positive ion) and an occupied electron state (negative ion) as these ions approach the metal surface. Because of the image charge effect, the levels broaden and shift in opposite directions towards the Fermi level of the metal. If and when there is overlap between the ion and the filled metal states, resonant electron transfer may occur, resulting in neutralization or ionization. E = energy axis, z = distance from surface, and Z_0 = apsis.

FIG. 5. Exit energies of O^-, O_2^-, and O_2^+ as a function of O^+ incidence energy on (a) Pd(O) and (b) Pt(O), respectively. The open symbols are experimental data. The solid lines are linear fittings with fixed slopes, calculated from binary collision theory applied to atomic (O^-) and molecular (O_2^-, O_2^+) ion exits. The intercepts indicate cumulative inelastic energy losses.

incident projectiles scatters without undergoing an ER reaction. The intercept of the O^- exit energy line fit, -12.04 eV, indicates additional inelastic energy losses. The kinematic factor for molecular O_2 scattering from Pd is calculated from Eq. (2) to be 0.6532, which captures the O_2^- exit energy data very well; see Fig. 5(a). Similarly, the O^- and O_2^- ion exit energy data for O^+/Pt, shown in Fig. 5(b), can be explained equally well by BCT with calculated kinematic factors of 0.8484 and 0.7933, respectively. Despite the weaker signal, the O_2^+ exit energy data on Pt can also be fitted with the latter kinematic factor. Note that, for scattering on Pd or Pt, both molecular ion products possess lower exit energy than the scattered O^-, as predicted by BCT (*vide supra*).

It is again useful to compare the energetics of the two molecular products, O_2^+ vs O_2^-. In contrast to N^+/Pd(O), where NO^+ exits the surface faster that NO^-, O^+/Pd(O) yields the *opposite* result: O_2^- is faster than O_2^+. Furthermore, ion yield is different: dynamic O_2^+ scattering signal is weak and noisy in comparison to the strong O_2^- signal. These observations can be explained by considering ionization processes for O_2 near the metal surface. The electron affinity and ionization energy of O_2 are 0.45 [30] and 12.07 eV [31], respectively, and both are larger than those for NO, favoring a higher negative ion yield. O_2^- ions are most likely formed by resonant electron attachment from the metal to O_2, which has an energy barrier ($\phi -$ EA) of 4.8 and 5.2 eV for Pd and Pt, respectively. These values are lower than the energy barriers for resonant ionization (IE $- \phi$) to form O_2^+ on Pd and Pt, which are 6.9 and 6.4 eV, respectively. The difference implies a greater energy penalty for forming O_2^+, consistent with the slower speed and yield of O_2^+ vs O_2^-. The measured inelastic energy loss for forming O_2^+ on Pt is about 5 eV greater than that for O_2^- [see Fig. 5(b)], suggesting that O_2^+ is formed by direct ionization through an electronic promotion during the hard collision, rather than resonant ionization.

*giapis@cheme.caltech.edu

[1] W. H. Weinberg, Acc. Chem. Res. **29**, 479 (1996).
[2] G. Ertl, Angew. Chem., Int. Ed. Engl. **47**, 2 (2008).
[3] J. Harris and B. Kasemo, Surf. Sci. **105**, L281 (1981).
[4] E. W. Kuipers, A. Vardi, A. Danon, and A. Amirav, Phys. Rev. Lett. **66**, 116 (1991).
[5] A. Danon and A. Amirav, J. Phys. Chem. **93**, 5549 (1989).
[6] C. T. Rettner, Phys. Rev. Lett. **69**, 383 (1992).
[7] C. T. Rettner and D. J. Auerbach, Phys. Rev. Lett. **74**, 4551 (1995).
[8] C. T. Rettner and D. J. Auerbach, Science **263**, 365 (1994).

[9] B. Jackson and M. Persson, J. Chem. Phys. **96**, 2378 (1992).
[10] E. R. Williams, G. C. Jones Jr., L. Fang, R. N. Zare, B. J. Garrison, and D. W. Brenner, J. Am. Chem. Soc. **114**, 3207 (1992).
[11] B. Jackson and D. Lemoine, J. Chem. Phys. **114**, 474 (2001).
[12] R. Pétuya, M. A. Nosir, C. Crespos, R. Díez Muiño, and P. Larrégaray, J. Phys. Chem. C **119**, 15325 (2015).
[13] M. Maazouz, T. L. O. Barstis, P. L. Maazouz, and D. C. Jacobs, Phys. Rev. Lett. **84**, 1331 (2000).
[14] C. L. Quinteros, T. Tzvetkov, and D. C. Jacobs, J. Chem. Phys. **113**, 5119 (2000).
[15] M. J. Gordon, X. Qin, A. Kutana, and K. P. Giapis, J. Am. Chem. Soc. **131**, 1927 (2009).
[16] T. Zaharia, A. W. Kleyn, and M. A. Gleeson, Phys. Rev. Lett. **113**, 053201 (2014).
[17] M. Blanco-Rey, E. Díaz, G. A. Bocan, R. D. Muiño, M. Alducin, and J. I. Juaristi, J. Phys. Chem. Lett. **4**, 3704 (2013).
[18] S. R. Kasi, H. Kang, C. S. Sass, and J. W. Rabalais, Surf. Sci. Rep. **10**, 1 (1989).
[19] J. Mace, M. J. Gordon, and K. P. Giapis, Phys. Rev. Lett. **97**, 257603 (2006).
[20] C. T. Campbell, G. Ertl, H. Kuipers, and J. Segner, Surf. Sci. **107**, 220 (1981).
[21] X. Guo, A. Hoffmann, and J. T. Yates, Jr., J. Chem. Phys. **90**, 5787 (1989).
[22] The intensity of the positive and negative ion signals cannot be quantitatively compared due to the unknown sensitivity of the channeltron.
[23] Using the velocity and geometry notation indicated in Fig. 2, the energy and momentum balances are as follows:

$$\frac{1}{2}m_P v_0{}^2 = \frac{1}{2}(m_P + m_A)v_e{}^2 + \frac{1}{2}m_S v_S{}^2$$
$$m_P v_0 = (m_P + m_A)v_e \cos\theta + m_S v_S \cos\varphi$$
$$(m_P + m_A)v_e \sin\theta = m_S v_S \sin\varphi.$$

[24] D. P. Smith, J. Appl. Phys. **38**, 340 (1967).
[25] See Supplemental Material http://link.aps.org/supplemental/10.1103/PhysRevLett.116.253202 for N^+ ion exits in N^+/Pd(O) and N^+/Pt(O), NO formation in N^+/Pt(O), and O_2 formation in O^+/Pd(O) and O^+/Pt(O).
[26] J. N. M. van Wunnik and J. Los, Phys. Scr. **T6**, 27 (1983).
[27] *CRC Handbook of Chemistry and Physics*, W. M. Haynes, 96th ed. (CRC Press and Taylor and Francis, Boca Raton, FL, 2016).
[28] C. A. Arrington, T. H. Dunning, Jr., and D. E. Woon, J. Phys. Chem. A **111**, 11185 (2007).
[29] In addition to charge transfer, there are other inelastic energy loss or gain mechanisms, such as internal excitation and bond cleavage or formation.
[30] K. M. Ervin, I. Anusiewicz, P. Skurski, J. Simons, and W. C. Lineberger, J. Phys. Chem. A **107**, 8521 (2003).
[31] R. G. Tonkyn, J. W. Winniczek, and M. G. White, Chem. Phys. Lett. **164**, 137 (1989).